# Anatomical Characteristics Contributing to Patellar Dislocations Following MPFL Reconstruction: A Dynamic Simulation Study

**Jeffrey C. Watts**
Department of Orthopedic Surgery,
Cleveland Clinic Akron General,
1 Akron General Avenue,
Akron, OH 44307
e-mail: wattsj3@ccf.org

**Lutul D. Farrow**
Orthopaedic & Rheumatologic Institute,
Cleveland Clinic Sports Health Center,
5555 Transportation Boulevard,
Garfield Heights, OH 44125
e-mail: farrowl@ccf.org

**John J. Elias**[1]
Department of Health Sciences,
Cleveland Clinic Akron General,
1 Akron General Avenue
Akron, OH 44307
e-mail: eliasj@ccf.org

*Pathologic anatomy is a primary factor contributing to redislocation of the patella following reconstruction of the medial patellofemoral ligament (MPFL). A pivot landing was simulated following MPFL reconstruction, with the hypothesis that position of the tibial tuberosity, depth of the trochlear groove, and height of the patella are correlated with lateral patellar maltracking. Thirteen dynamic simulation models represented subjects being treated for recurrent patellar instability. Simplified Hertzian contact governed patellofemoral and tibiofemoral joint reaction forces. Pivot landing was represented with and without an MPFL graft in place. Measurements related to patellar height (Caton-Deschamps index), trochlear groove depth (lateral trochlear inclination), and position of the tibial tuberosity (lateral tibial tuberosity to posterior cruciate attachment distance, or lateral TT-PCL distance) were measured from the models and correlated with patellar lateral shift with the knee extended (5 deg of flexion) and flexed (40 deg). The patella dislocated for all models without an MPFL graft and for two models with a graft represented. With an MPFL graft represented, patellar lateral shift was correlated with Caton-Deschamps index ($r^2 > 0.35$, $p < 0.03$) and lateral trochlear inclination ($r^2 \geq 0.45$, $p < 0.02$) at both 5 deg and 40 deg of flexion. For a simulated pivot landing with an MPFL graft in place, lateral patellar tracking was associated with a high patella (alta) and shallow trochlear groove. The study emphasizes the importance of simulating activities that place the patella at risk of dislocation when evaluating patellar stability.*
[DOI: 10.1115/1.4055886]

*Keywords: patellar instability, MPFL reconstruction, computational simulation*



## Introduction

Medial patellofemoral ligament (MPFL) reconstruction is currently the most common surgical approach for patellar stabilization following lateral patellar dislocation [1,2]. Continued instability following MPFL reconstruction is generally reported for less than 4% of patients [2,3], although rates as high as 8% to 20% have also been reported [4–8]. Anatomical risk factors, such as trochlear dysplasia, patella alta, or a laterally positioned tibial tuberosity, are commonly associated with poor outcomes following MPFL reconstruction [4,9–13]. A laterally positioned tibial tuberosity increases the lateral component of the force applied to the patella by the quadriceps muscles and patellar tendon, contributing to postoperative patellar maltracking. Patella alta and trochlear dysplasia reduce articular constraints that resist lateral maltracking, due to delayed entry of the patella into the trochlear groove during flexion and a shallow trochlear groove, respectively. MPFL reconstruction is typically considered for patients with limited pathologic anatomy. Higher levels of pathology are typically addressed with procedures such as tibial tuberosity realignment or deepening of the trochlear groove [1,14]. Some recent studies have advocated for broader use of MPFL reconstruction [15–17], in order to minimize surgical complications, postoperative pain, and recovery time associated with procedures including bone cuts.

Numerous computational and in vitro biomechanical studies have been performed to characterize patellar stability following MPFL reconstruction. These studies have primarily characterized patellar stability based on motion during simulated activities of daily living [18–20] or patellar shift in response to a laterally directed force [21–24]. Dynamic functional activities that place the knee at risk of patellar dislocation, such as multidirectional twisting [25,26], have yet to be represented, limiting the current understanding of how pathologic anatomy contributes to patellar dislocations following MPFL reconstruction.

The current study focuses on biomechanical function of MPFL grafts while preventing a patellar dislocation. The study uses computational simulation to represent knees being treated for patellar dislocation performing a dynamic pivot landing, while characterizing knee anatomy, graft tension, and patellofemoral kinematics. The hypothesis of the study is that pathologic anatomy related to a laterally positioned tibial tuberosity, trochlear dysplasia, and patella alta are correlated with lateral patellar tracking during a pivot landing. The study also compares graft function and patellofemoral kinematics between pivot landing and knee squatting, which is a stable activity more commonly used to assess patellar stability.

## Methods

**Computational Models of Subjects.** Computational models representing 13 knees about to undergo surgical patellar stabilization for recurrent lateral patellar instability were used to simulate pivot landing and knee squatting. The models were based on

[1]Corresponding author.
Manuscript received March 7, 2022; final manuscript received September 28, 2022; published online December 5, 2022. Assoc. Editor: Bruce MacWilliams.

  

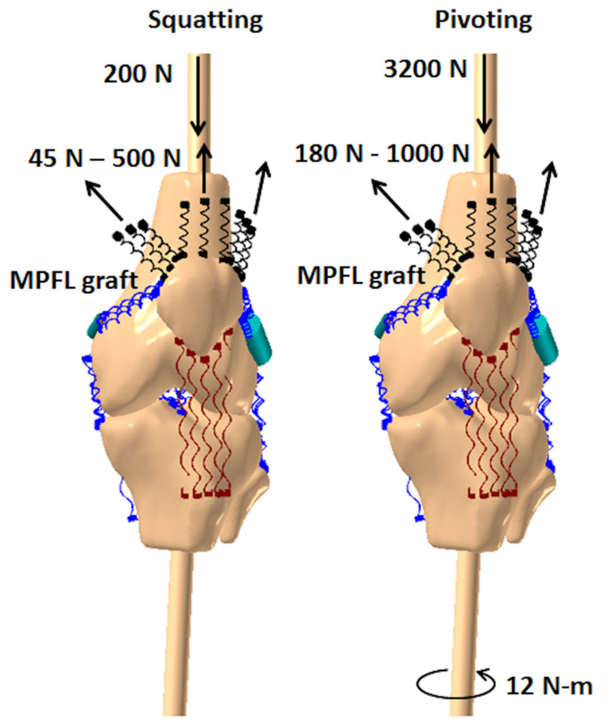


**Fig. 1 Computational model for multibody dynamic simulation of knee squatting and a pivot landing. The pivot landing was represented with a larger peak quadriceps force (1000 N), force at the hip (3200 N), and external tibial torque (12 N·m) than squatting.**

subjects ranging from 14 to 43 years old (mean = 22 years). For one of the knees, the tibial tuberosity had been surgically realigned to stabilize the patella prior to model development, but the subject experienced a subsequent dislocation. The local institutional review board provided approval for the study.

Accuracy of the computational output has been evaluated by comparison to data generated from subjects through a series of prior studies. For each computational model, an activity performed by the corresponding subject during diagnostic imaging was simulated for comparison to the kinematics data from the subjects. The activity was either knee extension against gravity during a dynamic CT scan [27] or isometric extension at multiple positions of knee flexion within an MRI scanner [28]. For fifteen models, root-mean-square errors measured over multiple flexion angles per subject were 2.5 mm and 4.0 deg for lateral patellar shift and tilt, respectively [20]. For a subgroup of patients with postoperative imaging, the average (±standard deviation) preoperative to postoperative (MPFL reconstruction or tibial tuberosity realignment) decrease in patellar lateral shift and tilt were 1.4 ± 3.8 mm and 2.5 deg ± 4.1 deg, respectively, for the subjects, compared to 2.4 ± 4.8 mm and 2.3 deg ± 5.9 deg for simulated motions [29]. A similar accuracy assessment for tibiofemoral kinematics reported root-mean-square errors of 5.5 deg and 1.8 mm for tibial external rotation and lateral shift, respectively [30].

**Simulation of Knee Motion.** Representation of knee function with the multibody dynamic simulation models (RecurDyn, FunctionBay, Seongnam, Korea) has been described in detail previously [20,29,30] (Fig. 1). Bones, cartilage surfaces, and soft tissue attachment points were reconstructed from MRI scans of the extended and unloaded knee (twelve 3.0 T and one 1.5 T, proton density weighted, slice thickness ranging from 0.5 mm to 3.0 mm). Cartilage surfaces and the underlying bones were treated as rigid bodies. Contact at the patellofemoral and tibiofemoral cartilage surfaces generated reaction forces based on simplified Hertzian contact [31–33] according to

$$F_c = k\delta^n + B(\delta)\delta' \tag{1}$$

where $F_c$ is the contact force in the cartilage, $k$ is the contact stiffness coefficient (1000 N/mm), $\delta$ is the penetration of surfaces, $\delta$' is the penetration velocity, $n$ is the compliance exponent (1.5), and B($\delta$) is the damping coefficient (5 N·s/mm).

Multiple tension-only springs were used to represent the medial and lateral collateral ligaments (three springs each), anterior and posterior cruciate ligaments (2), patellar tendon (5), posterior capsule (4), lateral retinaculum (2), and medial retinaculum minus the native MPFL (1). Properties for stiffness, damping, and prestrain at full extension were assigned based on previous publications [34–36]. Quadriceps forces were divided among the vastus medialis obliquus, vastus lateralis, and combination of the vastus intermedius, rectus femoris, and vastus medialis longus based on previous publications, with a weak vastus medialis obliquus represented by applying 5% of the total quadriceps force [37]. Quadriceps forces were applied through springs representing the quadriceps tendon.

An MPFL graft was represented for each knee. Each graft attached to the femur at the Schöttle point [38] and wrapped around the femoral condyle to the patellar attachment positioned between the medial edge of the vastus medialis obliquus attachment and the medial edge of the patella (Fig. 1). The portion from the wrapping surface to the patella was represented by two springs with a total stiffness of 20 N/mm to represent a dual strand gracilis tendon graft fixed to the femur [39]. An intra-operative technique was represented to set the resting length of the graft [6,40]. The knee was set at 30 deg of flexion. The patella was centered in the trochlear groove and shifted laterally by one-eighth of the medial-lateral width of the patella. The resting length was set to the length with the patella in the shifted position to avoid over constraining the patella [29]. The total force within the two springs, or graft tension, was quantified at each flexion angle during simulated function.

The models were used to simulate landing on one foot while turning toward the opposite foot (pivot landing) with and without an MPFL graft. Loading and boundary conditions representing a pivot landing were based on previous in vitro studies [41,42]. Motion was initiated with the knee at 5 deg of flexion. Forces were applied through the quadriceps and hamstrings muscles. The total quadriceps force increased from 180 N at 5 deg to 1000 N at 90 deg, while the medial and lateral hamstrings forces combined to apply 40% of the total quadriceps force. A force of 3200 N was applied at the hip to represent peak impulse force during landing (approximately four times body weight), and an external rotation torque of 12 N·m was applied to the tibia. Three rotational degrees-of-freedom were allowed at the ankle and flexion/extension, varus/valgus rotation, and superior/inferior translation allowed at the hip. Dual limb knee squatting was also simulated with an MPFL graft applied to represent a lower energy, uniplanar activity. Loading and boundary conditions were based on an in vitro knee simulator [43]. The total quadriceps force increased from 45 N at 5 deg to 500 N at 90 deg of flexion. A force of 200 N represented body weight applied to one hip, and no torque was applied to the tibia. The simulations used a Generalized-Alpha integrator with 200 time steps. Run time on a PC with a 2.5 GHz processor and 32 GB RAM was approximately 20 min.

**Characterization of Patellofemoral Kinematics and Anatomy.** Patellofemoral kinematics was quantified at every 5 deg of knee flexion. A local coordinate system was created for the femur based on the transepicondylar axis and long axis, with similar coordinate systems created for the patella and tibia, allowing characterization of knee kinematics based on the floating axis convention [44]. Analysis focused on patellar lateral shift and lateral tilt

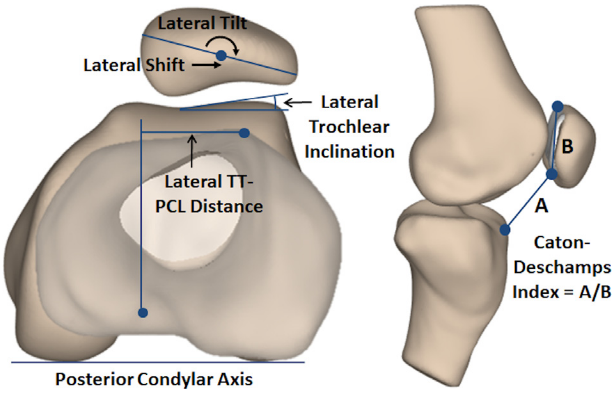


**Fig. 2 A computational model with landmarks and axes indicated to quantify parameters related to trochlear depth (lateral trochlear inclination), patellar height (Caton-Deschamps index), and position of the tibial tuberosity (lateral TT-PCL distance). The directions for patellar lateral shift and tilt are also shown. The tibia is partially transparent to show the PCL fossa.**

as measures related to patellar tracking with respect to the femur (Fig. 2).

Anatomical parameters related to lateral position of the tibial tuberosity, patella alta, and trochlear dysplasia were quantified for each model using automated algorithms. The anatomical parameters are related to alignment of multiple bones. To characterize these parameters based on motion without patellar dislocation, they were determined from squatting rather than pivoting, as described previously [20,45]. For trochlear dysplasia, depth of the trochlear groove was characterized based on lateral trochlear inclination with the knee at 5 deg of flexion (Fig. 2). Lateral trochlear inclination was measured within an axial plane perpendicular to the long axis of the patella, using a slice through the model that included the most anterior point of the lateral ridge of the groove. Lateral trochlear inclination was measured as the maximum slope of the lateral ridge of the trochlear groove with respect to the posterior condylar axis. The position of the tibial tuberosity was characterized at 5 deg of flexion. The lateral tibial tuberosity to posterior cruciate attachment (TT-PCL) distance was measured within the same plane used for lateral trochlear inclination. Lateral TT-PCL distance was measured from the midpoint of the patellar tendon attachment on the tibial tuberosity to the medial edge of the PCL attachment within the PCL fossa on the tibia, along the posterior condylar axis. Patella alta was characterized in terms of patellar height based on Caton-Deschamps index with the knee at 30 deg. Caton-Deschamps index was quantified within a sagittal plane as the ratio of the distance from a point on the distal edge of articular surface of the patella to the superior–anterior point on the tibia to the articular length along the patella.

**Statistical Analysis.** The primary analysis related patellar shift and tilt to anatomy with an MPFL graft in place for both a pivot landing and squatting. Linear regressions (SPSS, IBM, Armonk, NY) related patellar shift and tilt to anatomy with the knee extended (5 deg of flexion) and flexed to a position at which the patella should be captured by the trochlear groove (40 deg). Assumptions of normally distributed residuals were confirmed based on PP-plots and Shapiro–Wilks tests. Coefficients of determination ($r^2$), standardized beta ($\beta$) coefficients, and unstandardized $\beta$ coefficients with standard errors were quantified to evaluate the strength of the linear regressions. For standardized $\beta$ coefficients, dependent and independent variables are standardized to produce variances equal to 1, allowing comparisons between different anatomical factors for the influence on kinematics. For paired comparisons of patellar tracking and graft tension between pivoting and squatting, Shapiro–Wilks tests were performed to determine if the residuals of the comparisons were normally distributed, with a paired $t$-test or Wilcoxon signed-rank test used as needed. Statistical significance was set at $p < 0.05$.

## Results

Without an MPFL graft represented, the patella dislocated laterally during simulated pivot landing for all thirteen models. For two models, the patella also dislocated during pivoting with a graft represented. No patellar dislocations occurred during simulated squatting with an MPFL graft represented. Statistical analysis focused on early flexion (5 deg to 40 deg). The knee reached 40 deg of flexion without complete dislocation of the patella for all simulations with an MPFL graft represented.

Lateral patellar tracking was positively correlated with Caton-Deschamps index and negatively correlated with lateral trochlear inclination. Average values for Caton-Deschamps index, lateral trochlear inclination, and lateral TT-PCL distance were $1.2 \pm 0.3$, 15 deg $\pm 9$ deg, and $21 \pm 6$ mm. For pivoting and squatting, at 5 deg and 40 deg of flexion, patellar shift was significantly correlated with both Caton-Deschamps index and lateral trochlear inclination ($p < 0.04$, $r^2 > 0.3$) (Table 1). Standardized $\beta$ coefficients relating anatomy to lateral shift were 5%–12% larger for lateral trochlear inclination than Caton-Deschamps index, indicating

**Table 1 Significant correlations relating patellofemoral kinematics to anatomical parameters for simulated pivot landing and squatting with an MPFL graft represented**

| | | $p$-value | $r^2$ | Standardized $\beta$ | Unstandardized $\beta$ | Standard error $\beta$ |
|---|---|---|---|---|---|---|
| Pivot landing lateral shift (mm) | | | | | | |
| 5 deg | LTI (deg) | 0.012 | 0.45 | −0.67 | −0.58 mm/deg | 0.19 mm/deg |
| | CDI (mm/mm) | 0.026 | 0.38 | 0.61 | 18.4 mm | 7.2 mm |
| 40 deg | LTI (deg) | 0.004 | 0.55 | −0.74 | −0.69 mm/deg | 0.19 mm/deg |
| | CDI (mm/mm) | 0.008 | 0.49 | 0.70 | 22.3 mm | 6.9 mm |
| Pivot landing lateral tilt (deg) | | | | | | |
| 5 deg | LTI (deg) | 0.006 | 0.51 | −0.72 | −0.81 deg | 0.24 deg |
| 40 deg | LTI (deg) | 0.002 | 0.59 | −0.77 | −0.87 deg | 0.22 deg |
| Squatting lateral shift (mm) | | | | | | |
| 5 deg | LTI (deg) | 0.024 | 0.38 | −0.62 | −0.51 mm/deg | 0.19 mm/deg |
| | CDI (mm/mm) | 0.036 | 0.34 | 0.59 | 16.6 mm | 6.9 mm |
| 40 deg | LTI (deg) | 0.014 | 0.44 | −0.66 | −0.49 mm/deg | 0.17 mm/deg |
| | CDI (mm/mm) | 0.032 | 0.35 | 0.59 | 15.1 mm | 6.2 mm |
| Squatting lateral tilt (deg) | | | | | | |
| 5 deg | LTI (deg) | 0.007 | 0.50 | −0.71 | −0.82 deg | 0.25 deg |
| 40 deg | LTI (deg) | 0.032 | 0.35 | −0.60 | −0.56 deg | 0.23 deg |

LTI: lateral trochlear inclination; CDI: Caton-Deschamps index.

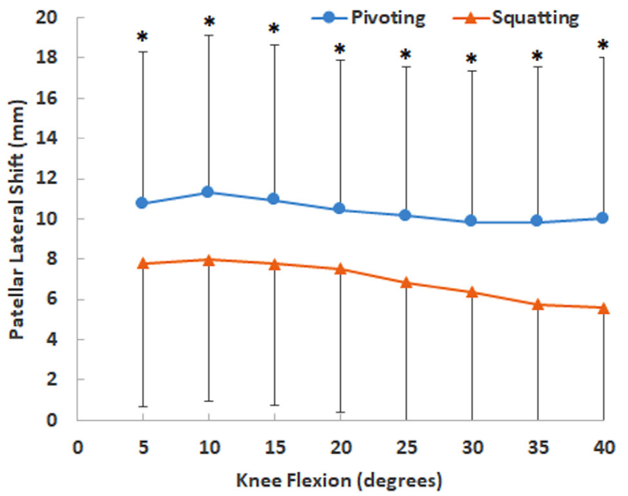


**Fig. 3 Average (±standard deviation) patellar lateral shift. A symbol (*) at a position of knee flexion indicates a significant difference between pivot landing and knee squatting.**

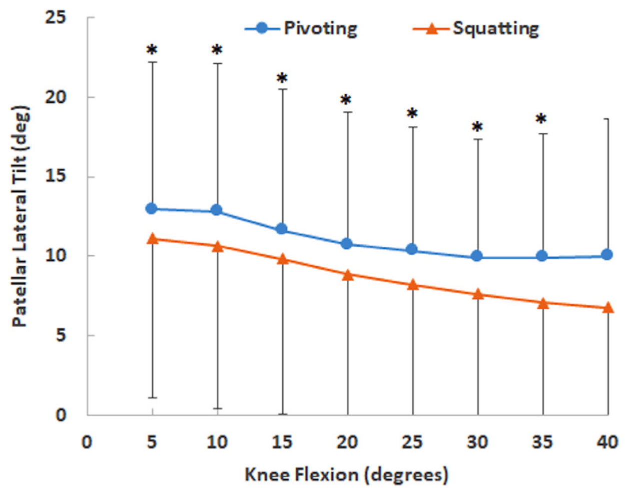


**Fig. 5 Average (±standard deviation) patellar lateral tilt. A symbol (*) at a position of knee flexion indicates a significant difference between pivot landing and knee squatting.**

lateral trochlear inclination was the primary parameter influencing patellar shift. The strongest correlations relating lateral shift to lateral trochlear inclination and Caton-Deschamps index occurred for pivoting at 40 deg ($r^2 \geq 0.49$, $|\text{standardized } \beta| \geq 0.7$). For pivoting and squatting, at both 5 deg and 40 deg, patellar tilt was significantly correlated with only lateral trochlear inclination ($p < 0.04$, $r^2 > 0.3$). The strongest correlation between lateral tilt and lateral trochlear inclination occurred for pivoting at 40 deg ($r^2 = 0.59$, $|\text{standardized } \beta| = 0.77$). No significant correlations were identified for lateral TT-PCL distance.

With an MPFL graft represented, patellar lateral shift and tilt were larger for pivot landing than squatting. The differences were statistically significant from 5 deg to 40 deg of flexion for patellar shift ($p < 0.001$, Fig. 3) and graft tension ($p < 0.01$, Fig. 4), and from 5 deg to 35 deg for tilt ($p < 0.05$, Fig. 5). Patellar lateral shift, lateral tilt, and graft tension peaked at 5 deg to 10 deg of knee flexion for pivoting and squatting. Average lateral shift was 3 to 4 mm larger for pivoting than squatting. Average lateral tilt was 1 deg to 3 deg larger for pivoting than squatting. Average graft tension peaked at approximately 50 N for pivoting, with the lowest value approximately 30 N. For squatting, average graft tension peaked at approximately 10 N and was minimal by 30 deg.

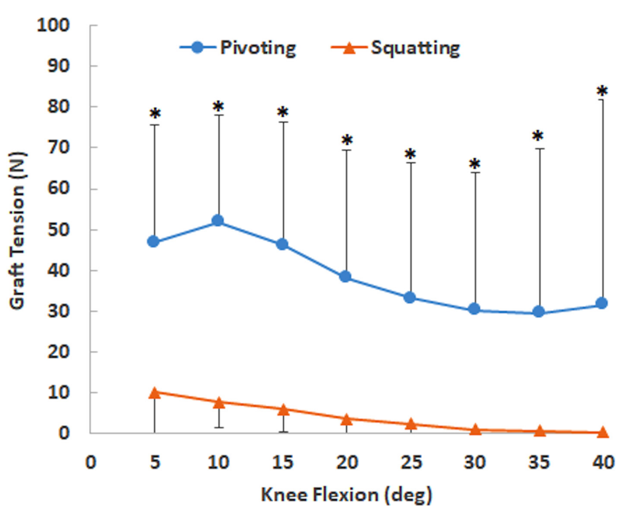


**Fig. 4 Average (±standard deviation) graft tension. A symbol (*) at a position of knee flexion indicates a significant difference between pivot landing and knee squatting.**

## Discussion

The results indicate patella alta and trochlear dysplasia are risk factors for patellar dislocation following MPFL reconstruction, especially for an activity including multidirectional twisting. During simulated pivoting, tension within an MPFL graft was sufficient to constrain the patella and initiate flexion, but the patella was not consistently captured by the trochlear groove as the knee flexed. For two knees, the patella started tracking lateral to the trochlear groove (large lateral shift) and completely dislocated beyond 40 deg of flexion. A large Caton-Deschamps index (patella alta that delays entry of the patella into the trochlear groove during flexion) and small lateral trochlear inclination (shallow trochlear groove) both limit the articular constraint resisting lateral patellar maltracking. Both parameters significantly influenced patellar lateral shift, with the strongest correlation occurring for lateral trochlear inclination with the knee at 40 deg. Based on the unstandardized $\beta$ coefficient, for pivoting at 40 deg, a 1 deg decrease in lateral trochlear inclination increases lateral patellar shift by approximately 0.7 mm. Also for pivoting at 40 deg, a 0.1 increase in Caton-Deschamps index (the increment typically used clinically) increases lateral patellar shift by approximately 2.2 mm. Similar to the current results, previous biomechanical studies that represented MPFL reconstruction identified a shallow trochlear groove and patella alta as factors that limit the constraint applied to the patella by the trochlear groove [21,45,46]. Lateral tilt was correlated with lateral trochlear inclination during simulated pivot landing, largely due to the lateral facet of the patella articulating along the lateral ridge of the trochlear groove.

For knee squatting, tension within an MPFL graft was sufficient to guide the patella into the trochlear groove at low flexion angles. As the patella was captured by the trochlear groove, articular constraints stabilized the patella, lateral tracking decreased, and graft tension dissipated. These trends have been noted for previous simulation studies [20,23,29]. Knee squatting produced lower values for patellar lateral shift and tilt and graft tension than pivoting, and no dislocations occurred. Kinematics differences between squatting and pivoting were more relevant for patellar shift than tilt, as the differences were larger than previously reported error levels for the simulations for lateral shift (2.5 mm), but not for lateral tilt (4.0 deg) [20]. The correlations relating lateral trochlear inclination and Caton-Deschamps index to patellofemoral kinematics were also weaker for squatting than pivoting. The differences between knee squatting and pivoting emphasize the importance of representing activities likely to cause patellar dislocation when evaluating surgical patellar stabilization.

The current study did not identify any statistically significant relationships between position of the tibial tuberosity and patellofemoral kinematics with an MPFL graft represented for either squatting or pivoting. A previous simulation study that evaluated knee squatting following MPFL reconstruction indicated patellar lateral shift was positively correlated with lateral TT-PCL distance [45], while an in vitro experimental study indicated lateralizing the tibial tuberosity increased lateral patellar tracking with an MPFL graft represented [47]. Lack of statistically significant correlations for the current study may be due to the experimental methods. The previous computational study represented lateral shift based on position within the trochlear groove (bisect offset index) instead of with respect to femoral reference frame along the transepicondylar axis and included variations between flexion angles within knees to identify significant correlations. The current study used the femoral reference frame to obtain normally distributed data for extreme values of lateral maltracking. The current study also focused on individual flexion angles. The knees used for the in vitro study did not reflect trochlear dysplasia or patellar alta associated patellar dislocations.

The computational approach uniquely represented MPFL reconstruction while simulating a dynamic activity that places the knee at risk of patellar dislocation. Dislocations during simulated squatting can be attributed to large forces applied by the quadriceps and patellar tendon, as well as external tibial rotation increasing the lateral orientation of the patellar tendon. By representing knees being treated for recurrent instability, the models also included representation of pathologic anatomy that contributes to patellar dislocations. The average Caton-Deschamps index was 1.2, which is considered borderline for patella alta [48,49]. The average lateral TT-PCL distance was 21 mm. The average TT-PCL distance for patients being treated for patellar instability is 22 mm when measured along the posterior tibial axis [50]. The posterior condylar axis was used for the current study to account for rotation of the tibia with respect to the femur. The average lateral trochlear inclination was 15 deg. The value was less than 11 deg for five knees, indicating trochlear dysplasia [51]. The lateral trochlear inclination values may also have been slightly higher than clinical measurements due to basing the computational measurements on maximum slope.

The dynamic simulation approach includes several limitations. The computational models were constructed based on manual segmentation of MRI scans, and generalized material properties were assigned based on previously published data, rather than individualized for the subjects. Also, menisci were not represented within the tibiofemoral joint. These limitations emphasize the importance of the previous accuracy assessments for the computational models. Representation of pivot landing includes some simplification. Pivoting on a planted foot was represented with an external torque applied to the tibia, with the analysis focused on early knee flexion. The approach allowed representation of pivoting with only quadriceps and hamstrings forces, similar to in vitro mechanical models representing pivoting [41,42]. The approach was sufficient to induce a dislocation for all models in the injured condition. The models only represented knees being treated for recurrent instability, so the correlations lack representation of less pathologic anatomy from healthy controls or knees that experienced only a single instability episode.

In conclusion, MPFL reconstruction is the preferred surgical approach for patellar stabilization to minimize surgical complications, postoperative pain, and recovery time. High energy, multiplanar activities such as a pivot landing place the knee at risk of patellar dislocation following MPFL reconstruction. Computational simulation demonstrated the potential for patellar dislocation during pivot landing despite MPFL reconstruction, emphasizing the importance of simulating activities that place the patella at risk of dislocation when evaluating patellar stability. The primary parameters associated with a risk of postoperative patellar dislocation were patella alta and a shallow trochlear groove.


## Funding Data

- Office of the Assistant Secretary of Defense for Health Affairs through the Peer Reviewed Medical Research Program (Award No. W81XWH2010040; Funder ID: 10.13039/100000090).


## Nomenclature

MPFL = medial patellofemoral ligament
TT-PCL = tibial tuberosity to posterior cruciate ligament attachment

## References


[1] Liu, J. N., Steinhaus, M. E., Kalbian, I. L., Post, W. R., Green, D. W., Strickland, S. M., and Shubin Stein, B. E., 2018, "Patellar Instability Management: A Survey of the International Patellofemoral Study Group," Am J. Sports Med., **46**(13), pp. 3299–3306.

[2] Schneider, D. K., Grawe, B., Magnussen, R. A., Ceasar, A., Parikh, S. N., Wall, E. J., Colosimo, A. J., Kaeding, C. C., and Myer, G. D., 2016, "Outcomes After Isolated Medial Patellofemoral Ligament Reconstruction for the Treatment of Recurrent Lateral Patellar Dislocations," Am. J. Sports Med., **44**(11), pp. 2993–3005.

[3] Shah, J. N., Howard, J. S., Flanigan, D. C., Brophy, R. H., Carey, J. L., and Lattermann, C., 2012, "A Systematic Review of Complications and Failures Associated With Medial Patellofemoral Ligament Reconstruction for Recurrent Patellar Dislocation," Am. J. Sports Med., **40**(8), pp. 1916–1923.

[4] Hopper, G. P., Leach, W. J., Rooney, B. P., Walker, C. R., and Blyth, M. J., 2014, "Does Degree of Trochlear Dysplasia and Position of Femoral Tunnel Influence Outcome After Medial Patellofemoral Ligament Reconstruction?," Am. J. Sports Med., **42**(3), pp. 716–722.

[5] Lind, M., Enderlein, D., Nielsen, T., Christiansen, S. E., and Faunø, P., 2016, "Clinical Outcome After Reconstruction of the Medial Patellofemoral Ligament in Paediatric Patients With Recurrent Patella Instability," Knee Surg. Sports Traumatol. Arthrosc., **24**(3), pp. 666–671.

[6] Lippacher, S., Dreyhaupt, J., Williams, S. R. M., Reichel, H., and Nelitz, M., 2014, "Reconstruction of the Medial Patellofemoral Ligament: Clinical Outcomes and Return to Sports," Am. J. Sports Med., **42**(7), pp. 1661–1668.

[7] Ronga, M., Oliva, F., Longo, U. M., Testa, V., Capasso, G., and Maffulli, N., 2009, "Isolated Medial Patellofemoral Ligament Reconstruction for Recurrent Patellar Dislocation," Am. J. Sports Med., **37**(9), pp. 1735–1742.

[8] Schiphouwer, L., Rood, A., Tigchelaar, S., and Koëter, S., 2017, "Complications of Medial Patellofemoral Ligament Reconstruction Using Two Transverse Patellar Tunnels," Knee Surg. Sports Med Arthrosc., **25**(1), pp. 245–250.

[9] Hiemstra, L. A., Kerslake, S., Loewen, M., and Lafave, M., 2016, "Effect of Trochlear Dysplasia on Outcomes After Isolated Soft Tissue Stabilization for Patellar Instability," Am. J. Sports Med., **44**(6), pp. 1515–1523.

[10] Kita, K., Tanaka, Y., Toritsuka, Y., Amano, H., Uchida, R., Takao, R., and Horibe, S., 2015, "Factors Affecting the Outcomes of Double-Bundle Medial Patellofemoral Ligament Reconstruction for Recurrent Patellar Dislocations Evaluated by Multivariate Analysis," Am. J. Sports Med., **43**(12), pp. 2988–2996.

[11] Nelitz, M., Williams, R. S., Lippacher, S., Reichel, H., and Dornacher, D., 2014, "Analysis of Failure and Clinical Outcome After Unsuccessful Medial Patellofemoral Ligament Reconstruction in Young Patients," Inter. Orthop., **38**(11), pp. 2265–2272.

[12] Valkering, K. P., Rajeev, A., Caplan, N., Tuinebreijer, W. E., and Kader, D. F., 2017, "An Evaluation of the Effectiveness of Medial Patellofemoral Ligament Reconstruction Using an Anatomical Tunnel Site," Knee Surg. Sports Med. Arthrosc., **25**(10), pp. 3206–3212.

[13] Wagner, D., Pfalzer, F., Hingelbaum, S., Huth, J., Mauch, F., and Bauer, G., 2013, "The Influence of Risk Factors on Clinical Outcomes Following Anatomical Medial Patellofemoral Ligament (MPFL) Reconstruction Using the Gracilis Tendon," Knee Surg. Sports Med. Arthrosc., **21**(2), pp. 318–324.

[14] Weber, A. E., Nathani, A., Dines, J. S., Allen, A. A., Shubin-Stein, B. E., Arendt, E. A., and Bedi, A., 2016, "An Algorithmic Approach to the Management of Recurrent Lateral Patellar Dislocation," J. Bone Jt. Surg. Am., **98**(5), pp. 417–427.

[15] Erickson, B. J., Nguyen, J., Gasik, K., Gruber, S., Brady, J., and Shubin Stein, B. E., 2019, "Isolated Medial Patellofemoral Ligament Reconstruction for Patellar Instability Regardless of Tibial Tubercle–Trochlear Groove Distance and Patellar Height: Outcomes at 1 and 2 Years," Am. J. Sports Med., **47**(6), pp. 1331–1337.

[16] Schlumberger, M., Schuster, P., Hofmann, S., Mayer, P., Immendörfer, M., Mayr, R., and Richter, J., 2021, "Midterm Results After Isolated Medial Patellofemoral Ligament Reconstruction as First-Line Surgical Treatment in Skeletally Immature Patients Irrespective of Patellar Height and Trochlear Dysplasia," Am J. Sports Med., **49**(14), pp. 3859–3866.

[17] Kim, J.-M., Sim, J.-A., Yang, H. Y., Kim, Y. M., Wang, J.-H., and Seon, J.-K., 2021, "Clinical Comparison of Medial Patellofemoral Ligament Reconstruction With or Without Tibial Tuberosity Transfer for Recurrent Patellar Instability," Am. J. Sports Med., **49**(12), pp. 3335–3343.

[18] Kaiser, P., Schmoelz, W., Schöttle, P. B., Heinrichs, C., Zwierzina, M., and Attal, R., 2019, "Isolated Medial Patellofemoral Ligament Reconstruction for Patella Instability is Insufficient for Higher Degrees of Internal Femoral Torsion," Knee Surg. Sports Med. Arthrosc., **27**(3), pp. 758–765.

[19] Philippot, R., Boyer, B., Testa, R., Farizon, F., and Moyen, B., 2012, "Study of Patellar Kinematics After Reconstruction of the Medial Patellofemoral Ligament," Clin. Biomech., **27**(1), pp. 22–26.

[20] Tanaka, M. J., Cosgarea, A. J., Forman, J. M., and Elias, J. J., 2021, "Factors Influencing Graft Function Following MPFL Reconstruction: A Dynamic Simulation Study," J. Knee Surg., **34**(11), pp. 1162–1169.

[21] Vinod, A. V., Hollenberg, A. M., Kluczynski, M. A., and Marzo, J. M., 2021, "Ability of Medial Patellofemoral Ligament Reconstruction to Overcome Lateral Patellar Motion in the Presence of Trochlear Flattening: A Cadaveric Biomechanical Study," Am. J. Sports Med., **49**(13), pp. 3569–3574.

[22] Spang, R., Egan, J., Hanna, P., Lechtig, A., Haber, D., DeAngelis, J. P., Nazarian, A., and Ramappa, A. J., 2020, "Comparison of Patellofemoral Kinematics and Stability After Medial Patellofemoral Ligament and Medial Quadriceps Tendon–Femoral Ligament Reconstruction," Am. J. Sports Med., **48**(9), pp. 2252–2259.

[23] Alvarez, O., Steensen, R. N., Rullkoetter, P. J., and Fitzpatrick, C. K., 2020, "Computational Approach to Correcting Joint Instability in Patients With Recurrent Patellar Dislocation," J. Orthop. Res., **38**(4), pp. 768–776.

[24] Ambra, L. F., Franciozi, C. E., Phan, A., Faloppa, F., and Gomoll, A. H., 2021, "Isolated MPTL Reconstruction Fails to Restore Lateral Patellar Stability When Compared to MPFL Reconstruction," Knee Surg. Sports Traumatol. **29**(3), pp. 793–799.

[25] Smith, T. O., Donell, S. T., Chester, R., Clark, A., and Stephenson, R., 2011, "What Activities Do Patients With Patellar Instability Perceive Makes Their Patella Unstable?," Knee, **18**(5), pp. 333–339.

[26] Atkin, D. M., Fithian, D. C., Marangi, K. S., Stone, M. L., Dobson, B. E., and Mendelsohn, C., 2000, "Characteristics of Patients With Primary Acute Lateral Patellar Dislocation and Their Recovery Within the First 6 Months of Injury," Am. J. Sports Med., **28**(4), pp. 472–479.

[27] Conry, K. T., Cosgarea, A. J., Tanaka, M. J., and Elias, J. J., 2021, "Influence of Tibial Tuberosity Position and Trochlear Depth on Patellar Tracking in Patellar Instability: Variations With Patella Alta," Clin. Biomech., **87**, p. 105406.

[28] Biyani, R., Elias, J. J., Saranathan, A., Feng, H., Guseila, L. M., Morscher, M. A., and Jones, K. C., 2014, "Anatomical Factors Influencing Patellar Tracking in the Unstable Patellofemoral Joint," Knee Surg Sports Traumatol. Arthrosc., **22**(10), pp. 2334–2341.

[29] Elias, J. J., Jones, K. C., Lalonde, M. K., Gabra, J. N., Rezvanifar, S. C., and Cosgarea, A. J., 2018, "Allowing One Quadrant of Patellar Lateral Translation During Medial Patellofemoral Ligament Reconstruction Successfully Limits Maltracking Without Overconstraining the Patella," Knee Surg. Sports Traumatol. Arthrosc., **26**(10), pp. 2883–2890.

[30] Elias, J. J., Rezvanifar, S. C., and Koh, J. L., 2022, "Groove-Deepening Trochleoplasty Reduces Lateral Patellar Maltracking and Increases Patellofemoral Contact Pressures: Dynamic Simulation," J. Orthop. Res., **40**(7), pp. 1529–1537.

[31] Guess, T. M., Liu, H., Bhashya, S., and Thiagarajan, G., 2013, "A Multibody Knee Model With Discrete Cartilage Prediction of Tibio-Femoral Contact Mechanics," Comput. Methods Biomech. Biomed Eng., **16**(3), pp. 256–270.

[32] Müller, J. H., Razu, S., Erdemir, A., and Guess, T. M., 2020, "Prediction of Patellofemoral Joint Kinematics and Contact Through Co-Stimulation of Rigid Body Dynamics and Nonlineal Finite Element Analysis," Comput. Methods Biomech. Biomed. Eng., **23**(11), pp. 718–733.

[33] Kwon, O. S., Purevsuren, T., Kim, K., Park, W. M., Kwon, T. K., and Kim, T. H., 2014, "Influence of Bundle Diameter and Attachment Point on Kinematic Behavior in Double Bundle Anterior Cruciate Ligament Reconstruction Using Computational Model," Comput. Math. Methods Med., **2014**, pp. 1–8.

[34] Blankevoort, L., Kuiper, J. H., Huiskes, R., and Grootenboer, H. J., 1991, "Articular Contact in a Three-Dimensional Model of the Knee," J. Biomech., **24**(11), pp. 1019–1031.

[35] Conlan, T., Garth, W. P., and Lemons, J. E., 1993, "Evaluation of the Medial Soft-Tissue Restraints of the Extensor Mechanism of the Knee," J. Bone Jt. Surg Am., **75**(5), pp. 682–93.

[36] Wismans, J., Veldpaus, F., Janssen, J., Huson, A., and Struben, P., 1980, "A Three-Dimensional Mathematical Model of the Knee-Joint," J. Biomech., **13**(8), pp. 677–685.

[37] Elias, J. J., Kilambi, S., Goerke, D. R., and Cosgarea, A. J., 2009, "Improving Vastus Medialis Obliquus Function Reduces Pressure Applied to Lateral Patellofemoral Cartilage," J. Orthop Res., **27**(5), pp. 578–583.

[38] Schöttle, P. B., Schmeling, A., Rosenstiel, N., and Weiler, A., 2007, "Radiographic Landmarks for Femoral Tunnel Placement in Medial Patellofemoral Ligament Reconstruction," Am. J. Sports Med., **35**(5), pp. 801–804.

[39] Saper, M. G., Meijer, K., Winnier, S., Popovich, J., Andrews, J. R., and Roth, C., 2017, "Biomechanical Evaluation of Classic Solid and All-Soft Suture Anchors for Medial Patellofemoral Ligament Reconstruction," Am. J. Sports Med., **45**(7), pp. 1622–1626.

[40] Marot, V., Sanchis-Alfonso, V., Perelli, S., Gelber, P. E., Sánchez Rábago, C. J., Ginovart, G., and Monllau, J. C., 2021, "Isolated Reconstruction of Medial Patellofemoral Ligament With an Elastic Femoral Fixation Leads to Excellent Clinical Results," Knee Surg. Sports Traumatol. Arthrosc.; **29**(3), pp. 800–805.

[41] Beaulieu, M. L., Wojtys, E. M., and Ashton-Miller, J. A., 2015, "Risk of Anterior Cruciate Ligament Fatigue Failure is Increased by Limited Internal Femoral Rotation During In Vitro Repeated Pivot Landings," Am. J. Sports Med., **43**(9), pp. 2233–2241.

[42] Oh, Y. K., Kreinbrink, J. L., Ashton-Miller, J. A., and Wojtys, E. M., 2011, "Effect of ACL Transection on Internal Tibial Rotation in an In Vitro Simulated Pivot Landing," J. Bone Jt. Surg. Am., **93**(4), pp. 372–80.

[43] Mizuno, Y., Kumagai, M., Mattessich, S. M., Elias, J. J., Ramrattan, N., Cosgarea, A. J., and Chao, E. Y. S., 2001, "Q-Angle Influences Tibiofemoral and Patellofemoral Kinematics," J. Orthop. Res., **19**(5), pp. 834–840.

[44] Grood, E. S., and Suntay, W. J., 1983, "A Joint Coordinate System for the Clinical Description of Three-Dimensional Motions: Application to the Knee," ASME J. Biomech. Eng., **105**(2), pp. 136–144.

[45] Elias, J. J., Jones, K. C., Rezvanifar, S. C., Gabra, J. N., Morscher, M. A., and Cosgarea, A. J., 2018, "Dynamic Tracking Influenced by Anatomy Following Medial Patellofemoral Ligament Reconstruction: Computational Simulation," Knee, **25**(2), pp. 262–270.

[46] Watson, N. A., Duchman, K. R., Grosland, N. M., and Bollier, M. J., 2017, "Finite Element Analysis of Patella Alta: A Patellofemoral Instability Model," Iowa Orthop. J., **37**, pp. 101–108.

[47] Stephen, J. M., Dodds, A. L., Lumpaopong, P., Kader, D., Williams, A., and Amis, A. A., 2015, "The Ability of Medial Patellar Kinematics and Contact Mechanics in the Presence of a Lateralized Tibial Tubercle," Am. J. Sports Med., **43**(9), pp. 2198–2207.

[48] Magnussen, R. A., De Simone, V., Lustig, S., Neyret, P., and Flanigan, D. C., 2014, "Treatment of Patella Alta in Patients With Episodic Patellar Dislocation: A Systematic Review," Knee Surg. Sports Med. Arthrosc., **22**(10), pp. 2545–2550.

[49] Woodmass, J. M., Johnson, N. R., Cates, R. A., Krych, A. J., Stuart, M. J., and Dahm, D. L., 2018, "Medial Patellofemoral Ligament Reconstruction Reduces Radiographic Measures of Patella Alta in Adults," Orthop. J. Sports Med., **6**(1).

[50] Heidenreich, M. J., Camp, C. L., Dahm, D. L., Stuart, M. J., Levy, B. A., and Krych, A. J., 2017, "The Contribution of the Tibial Tubercle to Patellar Instability: Analysis of Tibial Tubercle–Trochlear Groove (TT-TG) and Tibial Tubercle–Posterior Cruciate Ligament (TT-PCL) Distances," Knee Surg. Sports Med. Arthrosc., **25**(8), pp. 2347–2351.

[51] Batailler, C., and Neyret, P., 2018, "Trochlear Dysplasia: Imaging and Treatment Options," EFORT Open Rev., **3**(5), pp. 240–247.